



## Effects of zoledronic acid on osteoblasts in three-dimensional culture

Flora Thibaut, Tanguy Watrin, Fleur Meary, Sylvie Tricot, Virginie Legros,  
Pascal Pellen-Mussi, Dominique Chauvel-Lebret

### ► To cite this version:

Flora Thibaut, Tanguy Watrin, Fleur Meary, Sylvie Tricot, Virginie Legros, et al.. Effects of zoledronic acid on osteoblasts in three-dimensional culture. *Journal of medical and dental sciences*, 2015, 10 (1), pp.8-15. 10.1016/j.jds.2014.07.004 . hal-01088445

**HAL Id: hal-01088445**

**<https://hal.science/hal-01088445>**

Submitted on 11 Mar 2016

**HAL** is a multi-disciplinary open access archive for the deposit and dissemination of scientific research documents, whether they are published or not. The documents may come from teaching and research institutions in France or abroad, or from public or private research centers.

L'archive ouverte pluridisciplinaire **HAL**, est destinée au dépôt et à la diffusion de documents scientifiques de niveau recherche, publiés ou non, émanant des établissements d'enseignement et de recherche français ou étrangers, des laboratoires publics ou privés.

## Original Article

# EFFECTS OF ZOLEDRONIC ACID ON OSTEOBLASTS IN THREE-DIMENSIONAL CULTURE

Flora Thibaut,<sup>1,2,\*</sup> Tanguy Watrin,<sup>2,\*</sup> Fleur Méary,<sup>1,2</sup> Sylvie Tricot,<sup>2</sup> Virginie Legros,<sup>2</sup> Pascal Pellen-Mussi,<sup>2</sup> Dominique Chauvel-Lebret<sup>1,2,†</sup>

<sup>1</sup> Pôle d'odontologie et de chirurgie buccale, Centre Hospitalier Universitaire, Rennes, France

<sup>2</sup> Laboratoire de Biomateriaux en Site Osseux, UMR CNRS 6226 – Institut des Sciences Chimiques de Rennes, Faculté d'Odontologie, Université de Rennes 1, France

\* Both authors contributed equally to this work

† Corresponding author

Dominique Chauvel-Lebret

Laboratoire de Biomateriaux en Site Osseux, Faculté d'Odontologie, Université de Rennes 1, 2  
avenue du Pr. Léon Bernard, 35043 Rennes Cedex, France

Tel: +33 (0)2 23 23 43 64 / Fax: +33 (0)2 23 23 43 93

dominique.lebret-chauvel@univ-rennes1.fr

Running Title: Zoledronic acid effects on 3D-cultured osteoblasts

## ABSTRACT

**Background/purpose:** Bisphosphonates (BPs) are synthetic drugs with anti-tumour and bone antiresorptive activities. The use of BPs is suspected to favor the emergence of osteonecrosis of the jaw (ONJ), a putative side effect whose pathogenesis remains unclear. Thus, we aimed to get insights about the impact of BPs on osteoblasts functions, using a three-dimensional culture model, which is suggested to be more similar to the *in vivo* tissues than monolayers.

**Materials and methods:** Effects of low (0.1  $\mu\text{M}$ ) and high (10  $\mu\text{M}$ ) concentrations of zoledronic acid were investigated on osteoblasts (hFOB 1.19), cultured as multicellular spheroids (MCS). Proliferation, apoptosis, spheroid growth kinetics and morphology were studied using MTT and APH assays, Caspase 3 western-blotting, phase contrast imaging and scanning electron microscopy.

**Results:** Proliferation, apoptosis and spheroid morphology showed that 10  $\mu\text{M}$  ZA induced a significant reduction in the relative viable cell number, correlated with morphological alterations of spheroids and induction of apoptosis. On the opposite, lower ZA concentration (0.1  $\mu\text{M}$ ) promoted cell proliferation without affecting growth kinetics or spheroid morphology.

**Conclusion:** ZA sensitivity of osteoblasts depends on concentration and experimental models. The dual dose-dependent effects of ZA on osteoblasts cultured as spheroids, thereby promoting or inhibiting cell proliferation, may provide opportunities in tissue engineering. At last, hFOB spheroid culture system represents a valuable model for the exploration of the molecular basis of BPs action on osteoblasts and for the development and evaluation of implantable biomaterials in bone site.

**Keywords:** bisphosphonates (BPs), zoledronic acid (ZA), hFOB 1.19, multicellular spheroids (MCS), proliferation

## INTRODUCTION

Bisphosphonates (BPs) are synthetic compounds, both metabolically stable and structurally similar to inorganic pyrophosphate. They bind strongly to hydroxyapatite crystals and inhibit bone resorption by reducing physicochemical bone mineral dissolution and decreasing osteoclast activity. Due to their antiresorptive properties, these drugs are widely used in the clinical treatment of bone diseases with increased bone resorption such as post-menopausal osteoporosis, Paget's disease or lytic bone metastasis. (1) BPs can be divided into two groups depending on their molecular mechanism of action at the cellular level. (2) Simple BPs, such as clodronate and etidronate, are metabolized intracellularly to non-hydrolysable analogues of ATP. The accumulation of these metabolites in the cytosol of osteoclasts induces cell death, probably by inhibiting ATP-dependent intracellular enzymes. (3,4) The more potent amino-BPs (e.g., zoledronic acid (ZA), alendronate and ibandronate), which are not metabolized, alter osteoclast function by inhibiting enzymes of the mevalonate biosynthetic pathway, notably the farnesyl diphosphate synthase (FPPS). Inhibition of FPPS leads to depletion of the metabolites FPP and geranylgeranyl diphosphate necessary for the post-translational modification (prenylation) of small GTPases, thereby affecting subcellular localization and function of these signaling proteins essential for osteoclast survival and activity. (5)

BPs use has been linked to osteonecrosis of the jaw (ONJ), particularly in patients after intravenous therapy in the setting of malignancy. BPs-Related ONJ (BRONJ) can be caused by oral trauma or dental extraction, but it can also occur spontaneously. (6,7) Although causality between BPs exposure and ONJ is still controversial, a clinical staging system of BRONJ has been developed to more appropriately diagnose and clinically manage patients, ranging from stage 0 (no clinical evidence of necrotic bone, but non-specific clinical findings and symptoms) to stage 3 (exposed necrotic bone with pain, infection, pathologic fracture, extra oral fistula, oral



antral/oral nasal communication...). (8) Various hypotheses have been put forward to explain BRONJ pathophysiology, which is likely to be multifactorial. It is postulated that BRONJ localizes on the jaws because of the heavy bone turnover in this area, causing BPs to accumulate preferentially in jaws at cytotoxic concentrations. Pathophysiology may also involve suppression of bone turnover and angiogenesis, altered function of oral mucosal cells, microbial flora, anti-inflammatory effects and genetic predispositions. (9) Beyond well-described direct effects of BPs on osteoclastic activity, significant clinical and experimental evidence indicates that BPs also influence osteoblast functions. (10,11) *In vitro* and *in vivo* studies demonstrated dose-dependent effects of BPs on cell proliferation, cell differentiation, apoptosis and matrix mineralization. High concentrations ( $> 10 \mu\text{M}$ ) generally produce adverse effects on these processes that may account for the occurrence of BRONJ. (12-17) On the opposite, lower BPs concentrations act positively on osteoblastic function by promoting survival, proliferation and differentiation of bone-forming cells. (17-20) While this dual effect of BPs on osteoblasts is now well established, uncertainty remains concerning the threshold of cytotoxic and clinically relevant concentrations of BPs, probably because of multiple experimental models used for investigations.

The objective of this *in vitro* study was to evaluate the effects of ZA – a commonly prescribed amino-BPs – on osteoblasts in a three-dimensional (3-D) culture system, namely multicellular spheroids (MCS). (21) The MCS model is based on the cell's propensity to self-aggregate when cultured in non-adhesive conditions. By restoring cell-cell and cell-matrix interactions, this 3-D system more closely mimics living tissue than monolayer cultures do, (22,23) making MCS-based assays more predictive of *in vivo* response to drugs. By examination of cell proliferation, cellular apoptosis and spheroid morphology after ZA treatment, we demonstrated that the dual dose-dependent effect of ZA already observed in monolayer culture is conserved in these osteoblastic microtissue-like cultures.

## **MATERIALS AND METHODS**

### **Cell culture**

The human fetal osteoblast cell line hFOB 1.19 (hFOB) was purchased from ATCC. hFOB cells were maintained in a 1:1 mixture of phenol red-free DMEM/Ham's F-12 medium, supplemented with 10% fetal bovine serum, 100 IU/mL penicillin, 100 µg/mL streptomycin, 20 mM HEPES buffer, 2 mM L-glutamine and 300 µg/mL G418. For cell expansion, hFOB cells were incubated at 33.5 °C and 5% CO<sub>2</sub> and fed twice a week. On reaching 80% confluency they were passaged using 0.05% trypsin-0.02% EDTA.

### **Generation and culture of MCS**

Formation of hFOB spheroids was achieved using agarose-coated 96-well tissue culture plates (50 µL of 1.5% agarose in Phosphate-Buffered Saline (PBS). The seeding density was  $2 \times 10^3$  cells per well. After 96 h of incubation, spheroid cultures were treated by replacing 50% (=100 µL) of supernatant with normal medium or medium supplemented with ZA (Zometa<sup>®</sup>, Novartis, East Hanover, NJ, USA) diluted in PBS at 2X final concentration. Half of the supernatant was replaced every 2 or 3 days with drug-free or drug-supplemented medium to ensure constant culture conditions. hFOB MCS were incubated at 33.5 °C for all experiments.

### **MTT assay**

The relative growth of hFOB cells in monolayer was evaluated using the MTT (methyl-tetrazolium salt; 3[4,5-dimethyl-thiazoyl-2yl] 2,5-diphenyl-tetrazolium bromide) assay as previously described.(24) Briefly, hFOB cells were seeded in 96-well tissue culture plates in 200 µL medium per well. After 24 h, the cells were incubated with different ZA concentrations for 3 and 10 days. hFOB cells were then exposed to MTT (1 mg/mL) for 3 h at 37 °C. After complete solubilization of formazan crystals in DMSO, optical density was measured on an ELISA plate reader at 570 nm.

### **APH assay**

The relative cell proliferation of hFOB in 3-D culture was evaluated after 3 days and 10 days in absence or presence of 0.1 or 10  $\mu$ M ZA using the acid phosphatase assay (APH) as previously described. (25) Briefly, 10 spheroids from the same culture conditions were pooled, washed with PBS and transferred into a well of a 96-well microplate. The supernatant was discarded to a final volume of 100  $\mu$ L. Then, 100  $\mu$ L of the assay buffer (Immunopure p-nitrophenyl phosphate 20 mg/10 mL, sodium acetate 0.1 M, Triton X100, 0.1%) was added to each well, and plates were incubated at 37 °C for 90 min. Following incubation, 10  $\mu$ L of 1 N NaOH was supplemented to each well, and absorption at 405 nm was measured on an ELISA plate reader.

### **Microscopy analyses**

Phase-contrast imaging of hFOB MCS was performed using an inverted microscope. Spheroids were assessed visually for differences in cell morphology from day 0 (i.e., 96 h after spheroid initiation) to day 14, in absence or presence of ZA. At least 48 MCS from each indicated time point were used to calculate the average diameter using Photoshop<sup>®</sup> software. In addition, hFOB MCS cultivated for 3 days or 10 days in drug-free or drug-supplemented medium were examined by scanning electron microscopy (SEM). Spheroids were rinsed twice in PBS and fixed for 3 h with 2.5% glutaraldehyde in PBS. Then, samples were washed twice in PBS and dehydrated in graded alcohol (80°, 95° and 100°) and acetone. After critical drying point (CPD 010, Balzers Union, Balzers, Lichtenstein) using liquid carbon dioxide, samples were coated with a thin layer of gold-palladium and observed via SEM.

### **Protein extraction and Western blot analysis**

After 3 or 10 days of ZA treatment, hFOB MCS were collected, rinsed twice in cold PBS and homogenized in cold RIPA protein extraction buffer (50 mM Tris-HCl pH 7.4, 150 mM NaCl, 1% NP-40, 0.5% Na-deoxycholate, 0.1% SDS, 2 mM EDTA). Homogenates were then sonicated,

incubated on ice for 30 min and centrifuged at 14,000 g for 15 min at 4 °C. Supernatants (total protein) and pellets (cellular debris) were collected and stored at -80 °C until use. Proteins were quantified with the Micro BCA™ Protein Assay Kit (Thermo Scientific, Waltham, MA USA), according to the manufacturer's instructions. 20 µg of total proteins were separated by electrophoresis in a 10% polyacrylamide SDS gel and transferred onto a PVDF membrane (Millipore, Merck KGaA, Darmstadt, Germany). After saturation, membranes were incubated with rabbit monoclonal antibodies raised against cleaved caspase-3 or alpha-tubulin. HRP-conjugated secondary antibodies were used subsequently before ECL signal detection. All antibodies were purchased from Cell Signaling Technology.

### **Statistical analysis**

The data are expressed as means ± standard deviation (s.d.). All experiments were conducted in triplicate. Comparisons across multiple experimental groups were performed using a one-way analysis of variance (ANOVA) followed by PLSD Fisher test using StatView v5.0 software. The observed differences relative to a probability of  $P < 0.05$  were considered significant.

## RESULTS

### Effect of ZA on hFOB cell proliferation in monolayer and 3-D cultures

To test whether the culture model influences ZA sensitivity of hFOB cells, a comparative study of relative cell growth between monolayer and spheroid cultures was carried out.

Analysis of cell proliferation in hFOB monolayer culture was realized using MTT assay after 3 days or 10 days culture with different ZA concentrations (Figure 1). Results are documented relative to the respective untreated control (set to 100%). Exposure of hFOB to 0.1  $\mu\text{M}$  ZA did not alter cell proliferation when compared with control cells ( $101.7\% \pm 7.2\%$  at day 3,  $102.5\% \pm 5.5\%$  at day 10). In contrast, relative growth of hFOB cells in monolayer culture was significantly decreased after 3 days and 10 days in presence of 10  $\mu\text{M}$  ZA, respectively to  $87.4\% \pm 7.4\%$  ( $P < 0.0001$ ) and  $40.4\% \pm 9.7\%$  ( $P < 0.0001$ ) of untreated cells' growth.

To explore the sensitivity of hFOB cells to ZA treatment in 3-D cultures, the relative number of viable cells in hFOB MCS incubated in absence or presence of 0.1 or 10  $\mu\text{M}$  ZA was determined using the APH assay (Figure 2) in comparison with respective untreated control (set to 100%). No significant difference was found between experimental conditions at day 3 ( $104.3\% \pm 9.9\%$  for 0.1  $\mu\text{M}$ ,  $94.2\% \pm 8.4\%$  for 10  $\mu\text{M}$ ), whereas a lower relative viable cell number was observed after 10 days incubation in 10  $\mu\text{M}$  ZA ( $80.4\% \pm 12.3\%$ ;  $P < 0.0001$ ), in agreement with MTT assay results although growth inhibition appeared much more pronounced in monolayer cultures. On the other hand, 10 days treatment with 0.1  $\mu\text{M}$  ZA seemed to promote slightly hFOB cell proliferation ( $114.5\% \pm 9.0\%$ ;  $P < 0.0001$ ) only when cultured as MCS.

### Impact of ZA on hFOB MCS growth and morphology

Monitoring of ZA effects on hFOB MCS growth and morphology was achieved through a combination of phase-contrast imaging and SEM analysis. Spheroid growth kinetics as

determined through MCS diameter measurement (Figure 3, Figure 4) revealed a very gradual and linear increase of mean spheroid size when cultured in absence of ZA, from 280  $\mu\text{m}$  on day 0 to 405  $\mu\text{m}$  on day 14. A nearly identical growth curve was obtained with spheroids incubated with 0.1  $\mu\text{M}$  ZA, without any statistically significant difference in spheroid size at any time point. On the opposite, growth inhibition was evident for hFOB MCS treated with 10  $\mu\text{M}$  ZA. Indeed, the diameter increase was almost totally abrogated as soon as 3 days culture, the difference in diameter being highly significant at day 7 ( $P < 0.0001$ ) when compared with untreated MCS. Interestingly, spheroid size reached a stable plateau (around 290  $\mu\text{m}$ ) maintained for at least 14 days of culture. To test whether ZA-induced growth inhibition of hFOB spheroid was correlated with morphological alterations, SEM analysis was carried out at 3 days or 10 days culture in drug-free or drug-supplemented medium (Figure 5). Microscopic examination of untreated spheroids after 3 or 10 days showed a compact spherical architecture without any distinguishable osteoblast – except for the round-shaped detaching ones – indicating an extremely dense cellular network. At high magnification (x3000), the surface of the MCS displayed filamentous structures, suggestive of cell membrane protrusions. SEM micrographs of spheroids treated with 0.1  $\mu\text{M}$  ZA for 3 or 10 days, or with 10  $\mu\text{M}$  ZA for 3 days did not reveal any morphological difference with control spheroids. In contrast, the structural integrity of hFOB MCS incubated for 10 days with 10  $\mu\text{M}$  ZA appeared dramatically affected. Indeed, although spheroids conserved a spherical aspect, they were characterized by a highly irregular and grainy surface.

### **Immunodetection of the active form of caspase-3 during ZA treatment**

Because exposure to the highest concentration of ZA compromised hFOB growth kinetics and morphology, we further examined whether the caspase cascade was triggered in response to ZA by performing Western blot analysis of cleaved caspase-3 (Figure 6). Immunodetection on total protein extracts from treated and untreated hFOB MCS revealed the presence of the active form

of caspase-3 after 3 days incubation with 10  $\mu$ M ZA. Moreover, no electrophoretic band was detected at day 10, indicating a transient activation of the apoptotic cascade.

## DISCUSSION

While BPs are widely used in clinical practice for their bone antiresorptive action, accumulating evidence demonstrates that osteoclasts are not the only direct cellular targets of BPs and that these drugs affect as well the activity of bone-forming osteoblastic cells. The findings that BPs modulate expression of RANKL (receptor activator of NF-kappaB ligand) and osteoprotegerin in osteoblasts that may in turn indirectly interfere with differentiation and survival of osteoclasts highlight the complexity of BPs action on bone cells.(26,27) In this context, the clinical study of Recker and colleagues showing an increase of the mineral apposition rate in patients intravenously treated with ZA exemplifies the current view that BPs modulate both arms of bone remodelling. (28) However, the molecular mechanisms by which BPs regulate the activity of osteoblast is not completely understood.

As exposed above, literature data indicate that high (micromolar) concentrations of BPs compromise viability and function of osteoblastic cells whereas lower concentrations stimulate osteoblast proliferation/differentiation and inhibit osteoblast/osteocyte apoptosis. In line with these observations, we demonstrated that ZA treatment of hFOB MCS induces positive or negative effects on osteoblasts in a dose-dependent manner. The highest concentration (10  $\mu$ M) blocks cell proliferation, alters MCS morphology and induces apoptosis that might be partly responsible for the development of BRONJ, whereas the lowest (0.1  $\mu$ M) promotes slightly but significantly cell growth.

Our findings that 10  $\mu$ M ZA inhibits the increase of MCS diameter after three days of incubation, and that the size of MCS remains constant the following days, suggest ZA exerts a cytostatic effect on osteoblasts, as already shown in other cell types. (29,30) The transient activation of caspase cascade may signify that ZA has a pro-apoptotic effect as well but only on some sensitive cells. To test whether ZA-induced growth inhibition was correlated with induction of bone-



forming activities, von Kossa staining was performed but did not reveal any mineralized nodule (data not shown). We conclude that the non-proliferative state of hFOB cells is not associated with the differentiation process, in contrast with previous results obtained with hFOB monolayer cultures. (17,31) Further supporting the idea that 3-D MCS model presents specific properties conditioning the effect of ZA on osteoblastic cells, our results from MTT and APH assays showed that the anti-proliferative effect of high concentration of ZA is much more acute in monolayer than in MCS, suggesting a protective effect of the 3-D experimental condition. Emergence of a hypoxia-related mechanism of resistance inside the MCS may provide an explanation for this phenomenon, hypoxic conditions preventing the anti-proliferative and pro-apoptotic effects of amino-BPs on osteoblast-like cells. (32) Alternatively, limited penetration and diffusion of ZA within the MCS may confine the pharmacological action of ZA to the cells located in the outermost layer of the spheroid, reducing consequently the proportion of cells exposed to ZA in comparison with monolayer cultures. Further studies would greatly benefit from fluorescently labeled conjugates of amino-BPs, which may provide useful information on the gradient distribution of these drugs within MCS as well as on the mechanisms of cellular uptake and potential transcytosis. (33,34) Conversely, we have described that 0.1  $\mu$ M ZA moderately promotes cell growth of MCS. This anabolic effect on osteoblasts has been demonstrated for other amino-BPs and is thought to involve binding to and inhibition of protein tyrosine phosphatases. (35) However, why this proliferative effect is restricted to hFOB cells cultured as MCS remains to be solved.

Our observation that the biological response to ZA not only depends on the concentration but also on the experimental model, as already proposed, (36) emphasizes the great potential of MCS model as microtissue-like model for drug evaluation. (37) Indeed, the restoration of cell-cell and cell-matrix interactions confers to the MCS model structural and functional properties

physiologically more relevant than monolayer cultures, giving to MCS-based assays a better predictive value of *in vivo* drug efficacy. For these reasons, in cancer research, the MCS represents an incomparable system for drug screening and metastasis analysis, as an avascular tumor model reproducing the *in vivo* pathophysiology of tumor tissue. (37,38)

Also, the MCS constitutes a highly valuable research tool for tissue engineering with multiple applications in regenerative medicine. For example, Kelm and colleagues have generated vascularized macrotissues by assembling individual MCS coated with endothelial cells, and observed that these macrotissues were connected to the host's vascular system after *in vivo* implantation, illustrating the promising potential of heterotypic MCS as minimal building block for *ex vivo* generation of macrotissues. (39)

Concerning the specific field of bone tissue engineering, multiple therapeutic strategies based on direct (coating, incorporation) or indirect (adjunct therapy) association of BPs with scaffolds (bioactive glasses, hydroxyapatite scaffolds, implants) have been developed. (40) These applications rely on the mechanical and putative osteoconductive and osteoinductive properties of bone substitutes, in conjunction with the local or systemic delivery of BPs, to promote bone regeneration. In this context, the hFOB spheroid culture system represents a convenient *in vitro* model for studying the effects of BPs on osteoblasts, and may greatly contribute to our understanding of their mechanisms of action on bone cells in the context of both tissue-engineered bone regeneration and physiopathology of BRONJ.

Based on the hFOB MCS model, this study shows that ZA exerts dual dose-dependent effects on osteoblast functions in 3-D cultures, inducing MCS growth arrest and apoptosis at micromolar concentration, but promoting cell proliferation at a lower level. Besides constituting a model of choice for elucidating the mechanisms of action of BPs on osteoblast, the hFOB MCS culture

system may also be very useful in assessing the effects of new bone substitutes on bone-forming cells and, more generally, in screening potential therapeutic molecules. Nevertheless, further studies are needed to improve the physiological relevance of the MCS model, for example through the development of heterotypic spheroids mixing osteoblasts and endothelial cells. Such experimental models may not only contribute to *in vitro* molecular and cellular studies but also have great applications in tissue engineering, especially as building blocks for tissue reconstruction with autologous cells.

## **ACKNOWLEDGMENTS**

The authors thank Joseph Le Lannic (CMEBA, University of Rennes 1), the members of the H<sup>2</sup>P<sup>2</sup> core facility (H<sup>2</sup>P<sup>2</sup> – histopathology core facility IFR 140, Biogenouest, University of Rennes 1, Inserm), Céline Allaire (Faculty of Dental Surgery, University of Rennes 1) and Isabelle Renard-Derrien (SCELVA, University of Rennes 1) whose help and cooperation aided in the completion of this study.

## REFERENCES

1. Russell RG. Bisphosphonates: the first 40 years. *Bone* 2011;49:2-19.
2. Rogers MJ, Crockett JC, Coxon FP, Monkkonen J. Biochemical and molecular mechanisms of action of bisphosphonates. *Bone* 2011;49:34-41.
3. Frith JC, Rogers MJ. Antagonistic effects of different classes of bisphosphonates in osteoclasts and macrophages in vitro. *J Bone Miner Res* 2003;18:204-12.
4. Lehenkari PP, Kellinsalmi M, Napankangas JP et al. Further insight into mechanism of action of clodronate: inhibition of mitochondrial ADP/ATP translocase by a nonhydrolyzable, adenine-containing metabolite. *Mol Pharmacol* 2002;61:1255-62.
5. Coxon FP, Rogers MJ. The role of prenylated small GTP-binding proteins in the regulation of osteoclast function. *Calcif Tissue Int* 2003;72:80-4.
6. Ruggiero SL. Bisphosphonate-related osteonecrosis of the jaw: an overview. *Ann N Y Acad Sci* 2011;1218:38-46.
7. Borromeo GL, Tsao CE, Darby IB, Ebeling PR. A review of the clinical implications of bisphosphonates in dentistry. *Aust Dent J* 2011;56:2-9.
8. Ruggiero SL, Dodson TB, Assael LA, Landesberg R, Marx RE, Mehrotra B. American Association of Oral and Maxillofacial Surgeons position paper on bisphosphonate-related osteonecrosis of the jaws--2009 update. *J Oral Maxillofac Surg* 2009;67:2-12.
9. Reid IR, Cornish J. Epidemiology and pathogenesis of osteonecrosis of the jaw. *Nat Rev Rheumatol* 2012;8:90-6.
10. Bellido T, Plotkin LI. Novel actions of bisphosphonates in bone: preservation of osteoblast and osteocyte viability. *Bone* 2011;49:50-5.
11. Maruotti N, Corrado A, Neve A, Cantatore FP. Bisphosphonates: effects on osteoblast. *Eur J Clin Pharmacol* 2012;68:1013-8.

12. Acil Y, Moller B, Niehoff P, Rachko K, Gassling V, Wiltfang J, Simon MJ. The cytotoxic effects of three different bisphosphonates in-vitro on human gingival fibroblasts, osteoblasts and osteogenic sarcoma cells. *J Craniomaxillofac Surg* 2012;40:e229-35.
13. Basso FG, Turrioni AP, Hebling J, de Souza Costa CA. Effects of zoledronic acid on odontoblast-like cells. *Arch Oral Biol* 2013;58:467-73.
14. Orriss IR, Key ML, Colston KW, Arnett TR. Inhibition of osteoblast function in vitro by aminobisphosphonates. *J Cell Biochem* 2009;106:109-18.
15. Patntirapong S, Singhatanadgit W, Chanruangvanit C, Lavanrattanakul K, Satravaha Y. Zoledronic acid suppresses mineralization through direct cytotoxicity and osteoblast differentiation inhibition. *J Oral Pathol Med* 2012;41:713-20.
16. Pozzi S, Vallet S, Mukherjee S et al. High-dose zoledronic acid impacts bone remodeling with effects on osteoblastic lineage and bone mechanical properties. *Clin Cancer Res* 2009;15:5829-39.
17. Reinholz GG, Getz B, Pederson L, Sanders ES, Subramaniam M, Ingle JN, Spelsberg TC. Bisphosphonates directly regulate cell proliferation, differentiation, and gene expression in human osteoblasts. *Cancer Res* 2000;60:6001-7.
18. Corrado A, Neve A, Maruotti N, Gaudio A, Marucci A, Cantatore FP. Dose-dependent metabolic effect of zoledronate on primary human osteoblastic cell cultures. *Clin Exp Rheumatol* 2010;28:873-9.
19. Pan B, To LB, Farrugia AN et al. The nitrogen-containing bisphosphonate, zoledronic acid, increases mineralisation of human bone-derived cells in vitro. *Bone* 2004;34:112-23.
20. Plotkin LI, Manolagas SC, Bellido T. Transduction of cell survival signals by connexin-43 hemichannels. *J Biol Chem* 2002;277:8648-57.

21. Alno N, Jegoux F, Pellen-Mussi P, Tricot-Doleux S, Oudadesse H, Cathelineau G, De Mello G. Development of a three-dimensional model for rapid evaluation of bone substitutes in vitro: effect of the 45S5 bioglass. *J Biomed Mater Res A* 2010;95:137-45.
22. Lin RZ, Chang HY. Recent advances in three-dimensional multicellular spheroid culture for biomedical research. *Biotechnol J* 2008;3:1172-84.
23. Pampaloni F, Reynaud EG, Stelzer EH. The third dimension bridges the gap between cell culture and live tissue. *Nat Rev Mol Cell Biol* 2007;8:839-45.
24. van Meerloo J, Kaspers GJ, Cloos J. Cell sensitivity assays: the MTT assay. *Methods Mol Biol* 2011;731:237-45.
25. Friedrich J, Eder W, Castaneda J, Doss M, Huber E, Ebner R, Kunz-Schughart LA. A reliable tool to determine cell viability in complex 3-d culture: the acid phosphatase assay. *J Biomol Screen* 2007;12:925-37.
26. Pan B, Farrugia AN, To LB, Findlay DM, Green J, Lynch K, Zannettino AC. The nitrogen-containing bisphosphonate, zoledronic acid, influences RANKL expression in human osteoblast-like cells by activating TNF-alpha converting enzyme (TACE). *J Bone Miner Res* 2004;19:147-54.
27. Viereck V, Emons G, Lauck V, Frosch KH, Blaschke S, Grundker C, Hofbauer LC. Bisphosphonates pamidronate and zoledronic acid stimulate osteoprotegerin production by primary human osteoblasts. *Biochem Biophys Res Commun* 2002;291:680-6.
28. Recker RR, Delmas PD, Halse J et al. Effects of intravenous zoledronic acid once yearly on bone remodeling and bone structure. *J Bone Miner Res* 2008;23:6-16.
29. Cornish J, Bava U, Callon KE, Bai J, Naot D, Reid IR. Bone-bound bisphosphonate inhibits growth of adjacent non-bone cells. *Bone* 2011;49:710-6.

30. Ohnuki H, Izumi K, Terada M et al. Zoledronic acid induces S-phase arrest via a DNA damage response in normal human oral keratinocytes. *Arch Oral Biol* 2012;57:906-17.
31. Reinholz GG, Getz B, Sanders ES et al. Distinct mechanisms of bisphosphonate action between osteoblasts and breast cancer cells: identity of a potent new bisphosphonate analogue. *Breast Cancer Res Treat* 2002;71:257-68.
32. Moon MH, Seol JW, Seo JS et al. Protective effect of hypoxia on bisphosphonate-related bone cell damage. *Mol Med Rep* 2010;3:869-75.
33. Coxon FP, Thompson K, Roelofs AJ, Ebetino FH, Rogers MJ. Visualizing mineral binding and uptake of bisphosphonate by osteoclasts and non-resorbing cells. *Bone* 2008;42:848-60.
34. Kashemirov BA, Bala JL, Chen X et al. Fluorescently labeled risedronate and related analogues: "magic linker" synthesis. *Bioconjug Chem* 2008;19:2308-10.
35. Morelli S, Bilbao PS, Katz S, Lezcano V, Roldan E, Boland R, Santillan G. Protein phosphatases: possible bisphosphonate binding sites mediating stimulation of osteoblast proliferation. *Arch Biochem Biophys* 2011;507:248-53.
36. Cvinkl B, Agis H, Stogerer K, Moritz A, Watzek G, Gruber R. The response of dental pulp-derived cells to zoledronate depends on the experimental model. *Int Endod J* 2011;44:33-40.
37. Friedrich J, Seidel C, Ebner R, Kunz-Schughart LA. Spheroid-based drug screen: considerations and practical approach. *Nat Protoc* 2009;4:309-24.
38. Vinci M, Gowan S, Boxall F et al. Advances in establishment and analysis of three-dimensional tumor spheroid-based functional assays for target validation and drug evaluation. *BMC Biol* 2012;10:29.

39. Kelm JM, Djonov V, Ittner LM, Fluri D, Born W, Hoerstrup SP, Fussenegger M. Design of custom-shaped vascularized tissues using microtissue spheroids as minimal building units. *Tissue Eng* 2006;12:2151-60.
40. Cattalini JP, Boccaccini AR, Lucangioli S, Mourino V. Bisphosphonate-based strategies for bone tissue engineering and orthopedic implants. *Tissue Eng Part B Rev* 2012;18:323-40.



## FIGURE LEGENDS

**Figure 1. Relative cell growth of hFOB cells in 2-D culture.** Relative growth of hFOB cells in monolayer culture was determined using a MTT assay after 3 days (D3) or 10 days (D10) of treatment with indicated concentrations of ZA. Number of viable cells is presented as percent of PBS-treated control spheroids (Ctrl), expressed as mean  $\pm$  s.d. of triplicate experiments (\*\*,  $P < 0.0001$  compared to control).

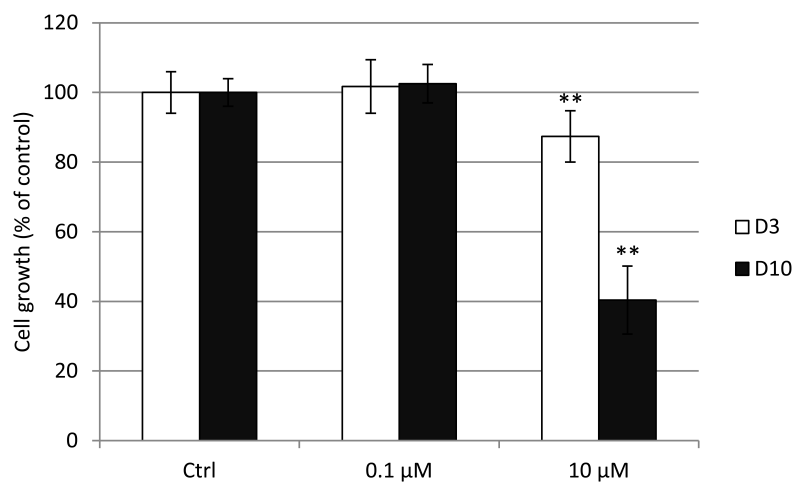


**Figure 2. Relative cell growth of hFOB cells in 3-D culture.** Relative cell growth in hFOB MCS was determined using an APH assay following 3 days (D3) or 10 days (D10) of treatment with indicated concentrations of ZA. Results are presented as percent of APH activity in PBS-treated control spheroids (Ctrl), expressed as mean  $\pm$  s.d. of triplicate experiments (\*\*,  $P < 0.0001$  compared to control).

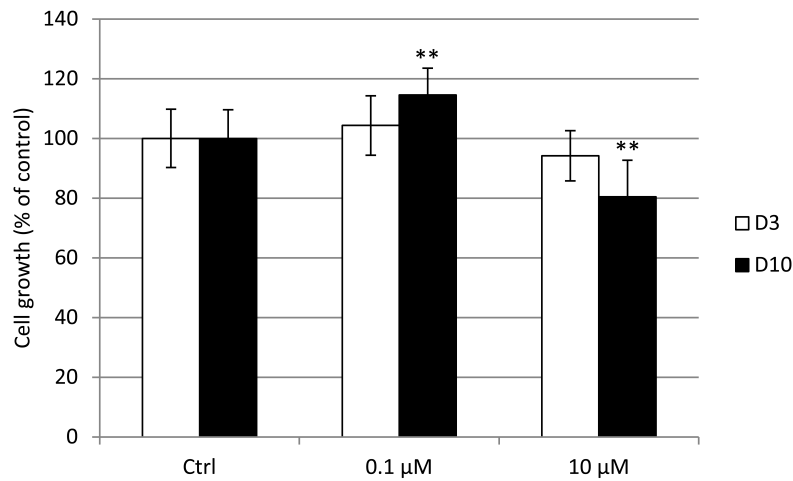


**Figure 3. Monitoring of hFOB MCS growth.** Graph visualizes spheroid diameter evolution kinetics of hFOB MCS grown in absence of ZA ( $\square$ ) or incubated with 0.1  $\mu\text{M}$  ( $\Delta$ ) or 10  $\mu\text{M}$  ( $\bullet$ ) ZA for up to 14 days. Data points are mean diameter  $\pm$  s.d. from 48 individual spheroids (\*\*,  $P < 0.0001$  compared to control).

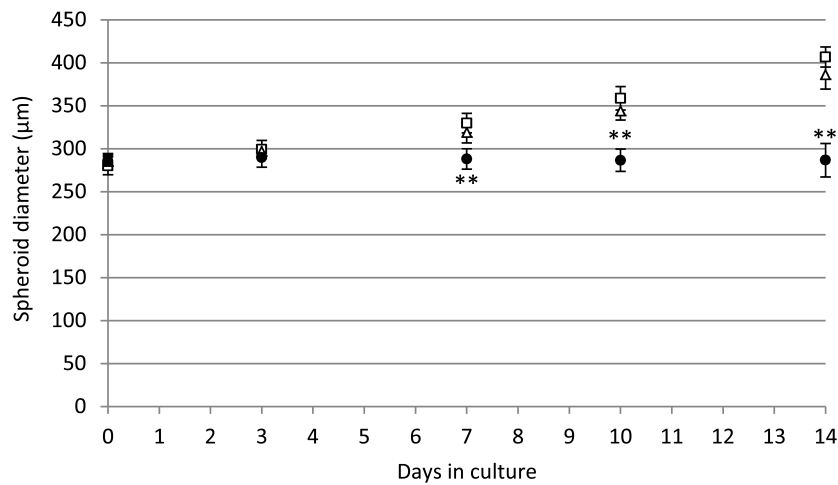


**Figure 4. Phase-contrast imaging of hFOB MCS.** Representative phase-contrast images of hFOB MCS are shown, illustrating the inhibitory effect of 10  $\mu\text{M}$  ZA on spheroid growth. Scale bar, 100  $\mu\text{m}$ .

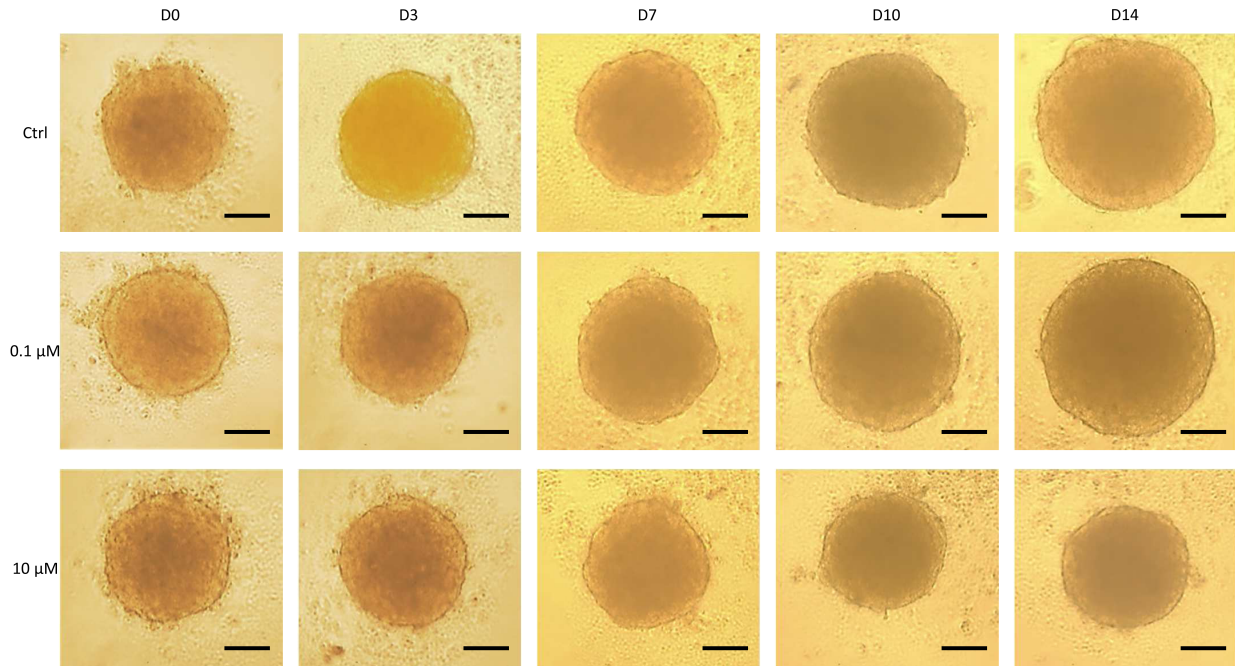


**Figure 5. Examination of hFOB MCS structural integrity by scanning electron microscopy (SEM).** SEM micrographs of hFOB MCS incubated for 3 days (A, D, G) or 10 days (B, C, E, F, H, I) in absence or presence of indicated ZA concentrations are shown. C, F and I correspond to high-magnification (x3000) images of insets in B, E and H respectively. Scale bars, 10 μm.

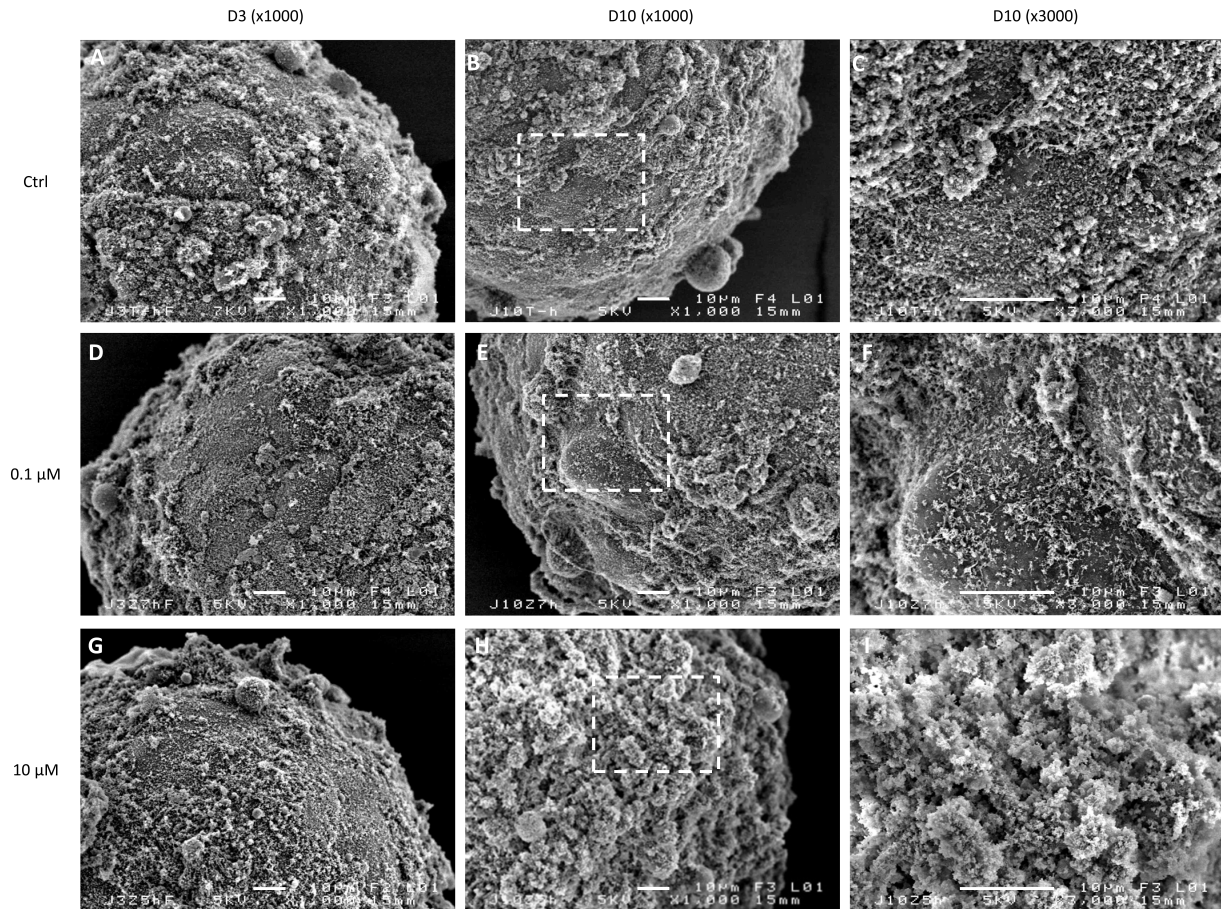


**Figure 6. Western blot analysis of cleaved caspase-3 in hFOB MCS upon treatment with ZA.** Protein level of the active form of caspase-3 was investigated in control spheroids or spheroids exposed to 0.1 or 10  $\mu$ M ZA during 3 or 10 days. Tubulin was used as a loading control.

